Orientational and structural order in strongly interacting dipolar hard spheres

D. Levesque and J. J. Weis
Laboratoire de Physique Théorique et Hautes Energies, Université de Paris XI, Bâtiment 211, 91405 Orsay Cedex, France
(Received 15 February 1994)

We show, by performing Monte Carlo simulations along a low temperature isotherm, that the structural behavior of a system of dipolar hard spheres transforms from a chainlike association at low density to a ferroelectric ordering at high density. The influence of the temperature variation and the dependence on boundary conditions are investigated.

PACS number(s): 61.20.Ja, 61.25.Em, 75.50.Mm

I. INTRODUCTION

Recent computer simulations have provided new insight into the structural and orientational behavior of strongly interacting dipolar hard and soft spheres [1–7]. The main conclusions of these calculations can be summarized as follows.

(1) At sufficiently low temperatures a *dense* system of dipolar hard spheres (or soft spheres) can spontaneously break its symmetry and order into a ferroelectric state [1–4]. Polarized domains form in the presence of a depolarizing field [1,4].

(2) No evidence is obtained for the existence of a gas-liquid transition in a broad density-temperature range in contrast with general belief and a variety of theoretical predictions [6,7].

(3) Instead the particles are found to associate into chainlike structures with near contact of the hard spheres and head-to-tail alignment of the dipole moments [5,7].

The purpose of the present paper is to present our preliminary Monte Carlo (MC) results [5] on chain formation in dipolar hard spheres (DHS) in more detail, to extend the results over a wider range of densities, and to reconsider the conclusions in the light of simulations with improved statistics. In Sec. II we briefly recall some of the details of the Monte Carlo calculations, in particular, the choice of the boundary conditions. Section III presents results for the structural behavior as a function of density for one isotherm and discusses the influence of boundary conditions and temperature variation. A summary and conclusions are given in Sec. IV.

II. MONTE CARLO SIMULATIONS

Most of the MC simulations were performed in the canonical (NVT) ensemble for a system of $N=500$ particles in a cubic box repeated periodically in space. A few additional runs using 128 particles allowed for more extended sampling of configuration space. The long range dipolar interactions were accounted for by using the Ewald method [8]. For an expression of the Hamiltonian of the system and full technical details, we refer the reader to Ref. [4]. Here we only briefly recall that the Hamiltonian splits into two terms, one having periodic symmetry and the other, of expression $2\pi\mathbf{M}^2/[(2\epsilon'+1)V]$ ($\mathbf{M}$ is the total dipole moment of the simulation cell and V is the volume), representing the contribution of a dielectric continuum of dielectric constant ϵ' surrounding a large sphere of periodic replica of the simulation cell.

Most of our calculations were performed for a periodic system ($\epsilon'=\infty$, no surface boundary) but, to test the influence of boundary conditions, a few additional calculations were carried out for $\epsilon'=1$ (vacuum). An alternative is to use "spherical boundaries" for which a large number of particles ($N=2046$) is confined to the inside of a spherical volume, an infinitely repulsive interaction between the sphere's surface and the particles preventing their escape. In this case the dipolar interactions extend between all particles of the system.

Sampling of phase space was made in the standard way, a Monte Carlo trial move consisting of displacement of the hard sphere center and rotation of its dipole moment. At low density (and low temperature) the acceptance ratio of a move was 0.15–0.20, a value which is still sufficient taking into account the average value of the attempted displacement ($\sim 0.1\sigma$) for the spheres to diffuse over a distance of the order of the length of the simulation cell within a run of 10^4–10^5 moves per particle.

III. RESULTS

Most of our simulation results are obtained along the isotherm $T^*=1/\mu^{*2}=0.0816$ ($\mu^*=3.5$) by varying the density $\rho^*=\rho\sigma^3$ from 0.005 to 0.80 [$\mu^*=(\mu/kT\sigma^3)^{1/2}$; μ is the dipole moment, T the temperature, k the Boltzmann constant, and σ the hard sphere diameter]. This value of the reduced dipole moment is typical of those encountered, for instance, in ferromagnetic colloids at room temperature [9]. In addition, the influence on the structural behavior of an increase of temperature (from 0.0816 to 0.25) was investigated at the two densities $\rho^*=0.1$ and 0.3. A distinctive feature of the present calculations compared to those already presented in Ref. [5] lies in the augmented statistics of the runs attaining typically $(1-3)\times 10^5$ trial moves per particle for the 500 particle system and 2×10^6 trial moves per particle for the 128 particle system. A summary of the thermodynamic properties and order parameters of the various state points considered is given in Table I. We can note that

TABLE I. Thermodynamic properties of dipolar hard spheres as a function of density and temperature (results complementary to those given in Table I of Ref. [5]). U_d/NkT is the dipolar energy, Z the compressibility factor, S the order parameter, and P the polarization. (a) Initial condition with random distribution of the dipole moments and (b) initial condition with perfect alignment of the dipole moments.

ρ^*	T^*	Boundary condition	N	Trial moves per particle	U_d/NkT	Z	S	P
0.005	0.0816	∞	500	100 000	−24.1	−0.10	0.06	0.09
0.01	0.0816	∞	500	140 000	−24.4	0.05	0.05	0.10
0.01	0.0816	∞	128	2 600 000	−25.6	−0.01	0.19	0.18
0.02	0.0816	∞	500	130 000	−24.7	0.10	0.05	0.05
0.05	0.0816	∞	500	100 000	−25.7	−0.01	0.06	0.10
0.05	0.0816	∞	128	2 000 000	−26.1	0.07	0.15	0.03
0.05	0.0816	Sphere	2046	70 000	−25.3		0.10	0.04
0.1	0.0816	∞	500	300 000	−26.2	−0.05	0.10	0.40
0.1	0.0816	1	500	100 000	−25.7	−0.07	0.07	0.02
0.1	0.25	∞	500	300 000	−3.87	0.33	0.04	0.03
(a) 0.4	0.0816	∞	500	110 000	−26.8	−0.06	0.04	0.04
(b) 0.4	0.0816	∞	500	110 000	−27.0	0.33	0.35	0.70
0.5	0.0816	∞	128	2 000 000	−27.4	0.31	0.46	0.02
(a) 0.6	0.0816	∞	500	110 000	−27.4	0.22	0.39	0.25
(b) 0.6	0.0816	∞	500	110 000	−27.9	−0.33	0.60	0.84
0.8	0.0816	∞	500	80 000	−28.5	0.15	0.57	0.83

for all thermodynamic states considered, the compressibility factor $Z = p/\rho kT$ (p is the pressure) is nearly zero.

A. Isotherm $T^* = 0.0816$

Since the structural behavior of the DHS is found to be qualitatively different on the low and high density sides of the isotherm, it will be convenient, for presentation of the results, to consider three separate density domains. It should be clear, however, that by introducing this division, we do not imply that they delimit thermodynamically stable phases.

1. $\rho^* \leq 0.2$

In this density domain, association of the DHS into long chainlike structures is most clearly apparent (cf. Figs. 1–4 which show snapshots of configurations of the system at densities $\rho^* = 0.01$, 0.05, 0.1, and 0.2). The aspect of these chains is very similar to that of partially flexible polymers. In fact, such a structure has been predicted, by de Gennes and Pincus [9] using qualitative arguments, to occur in ferromagnetic colloids.

To be able to make precise statements about the characteristics of the chains, an operational definition is required. Such a definition is clearly not unique and may be based on either a proximity or an energy criterion. The latter serves our purpose best since, in addition to proximity, it readily takes into account the fact that neighboring particles have their dipole moments roughly aligned with the direction of the vector joining the molecular centers. Two spheres were considered to be bound if their potential energy was less than a predetermined value $U_c = -1.4\mu^{*2}$ (i.e., 70% of the lowest energy of a pair of DHS at contact).

This choice of U_c was guided by the analysis of a number of instantaneous configurations of the system and a record of the average values of the first, second, and third lowest pair energies $\bar{E}_1$, $\bar{E}_2$, and $\bar{E}_3$ of each particle. When aggregation occurred, the values of $\bar{E}_1$ and $\bar{E}_2$ were close but considerably lower than $\bar{E}_3$, indicating chain formation rather than formation of more compact clusters (in which case all three values of $\bar{E}$ would have

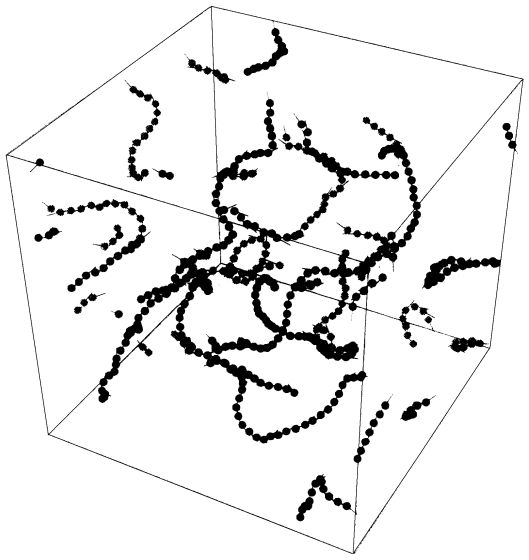

FIG. 1. Three-dimensional graph of an instantaneous configuration of 500 dipolar hard spheres at $\rho^* = 0.01$ and $T^* = 0.0816$ after 1.4×10^5 trial moves per particle. Hard spheres belonging to chains of length larger than 20 are represented in black, the others in gray. The direction of the dipole moment is indicated by a thin line. The box length is $L = 36.84\sigma$.

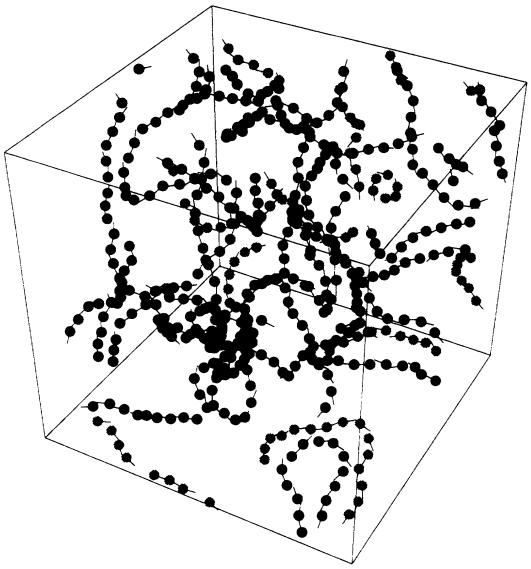

FIG. 2. Same as Fig. 1 but for $\rho^*=0.05$ (10^5 trial moves per particle). The box length is $L=21.54\sigma$. Hard spheres belonging to chains of length larger than 50 are represented in black, the others in gray.

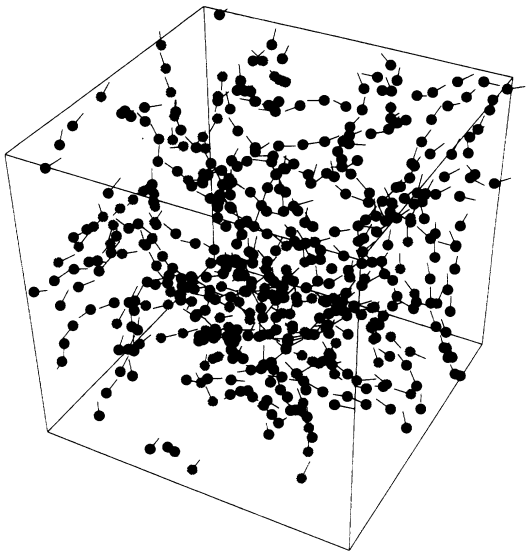

FIG. 4. Same as Fig. 1 but for $\rho^*=0.2$ (4×10^4 trial moves per particle). Hard spheres belonging to chains of length larger than 30 are represented in black, the others in gray. The box length is 13.57σ.

been close). For example, at $\rho^*=0.1$, $\mu^*=3.5$, one finds $\bar{E}_1=-22.16$, $\bar{E}_2=-19.17$, and $\bar{E}_3=-3.56$.

Chains were then identified as follows: For each particle i, in a given configuration, denote by $E_{ij}^{(1)}$ and $E_{ik}^{(2)}$ the energies of the pairs (i,j) and (i,k) having the first and second lowest energies. Choose a particle at random, say, i, and assume that it does not yet belong to a chain. If $E_{ij}^{(1)}<U_c$, particle j will belong to the chain. Move to particle j. If $E_{jl}^{(1)}<U_c$, particle l is accepted as the next member of the chain provided it does not yet belong to it or to another chain. Otherwise, the energy criterion is checked for $E_{jm}^{(2)}$. The process is continued until the chain stops (the energy criterion not satisfied or the neighbor belonging already to a chain). Then move back to the initial particle i and check the energy criterion for $E_{in}^{(2)}$ (second lowest pair energy) in order to grow the chain in the opposite direction. We note that the preceding chain definition, based on consideration of only the first two lowest pair energies, obviously does not allow for branched chain configurations. In fact, in the density region over which the chain concept seems meaningful, such configurations would occur only very rarely.

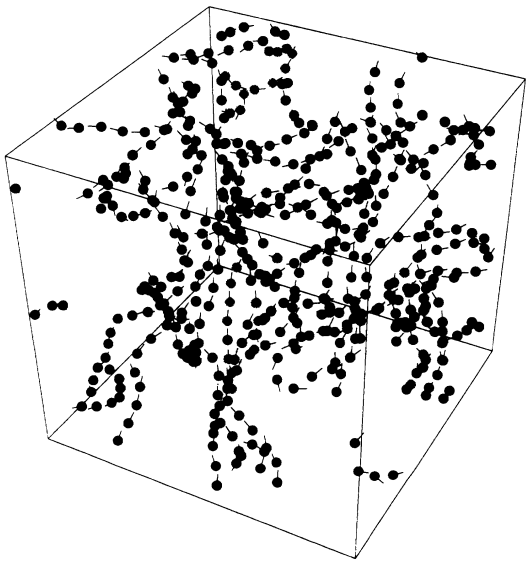

FIG. 3. Same as Fig. 1 but for $\rho^*=0.1$ (3×10^5 trial moves per particle). Hard spheres belonging to chains of length larger than 50 are represented in black, the others in gray. The box length is 17.1σ.

We can now define a chain length as the number of spheres belonging to a chain. Furthermore, it will be convenient to introduce two average lengths, one being the mean chain length in a given configuration defined as

$$l=\sum_s sn_s \Big/ \sum_s n_s \ , \tag{1}$$

where n_s is the number of chains having length s, and the second, denoted by an overbar, its average over configuration space, i.e.,

$$\bar{l}=\langle l \rangle \ . \tag{2}$$

Alternative expressions, which weight more heavily the longer chains, can also be used. These are defined as

$$l_s=\sum_s s^2 n_s \Big/ \sum_s sn_s \tag{3}$$

and

$$\bar{l}_s=\langle l_s \rangle \ . \tag{4}$$

However, if not specified explicitly, we will refer to

Eqs. (1) and (2) for the chain length. The flexibility of the chains will be characterized by an (instantaneous) mean persistence length

$$l_p = \frac{1}{\sigma} \sum_{\text{all chains with } s>10} \sum_{k=1}^{s-2} \mathbf{e}_1 \cdot \mathbf{e}_{1+k} \Big/ \sum_{s>10} n_s \qquad (5)$$

(l_p is the mean value for all chains with length larger than 10) and its average over configuration space

$$\bar{l}_p = \langle l_p \rangle \ . \qquad (6)$$

In Eq. (5), $\mathbf{e}_i = \mathbf{r}_{i+1} - \mathbf{r}_i$ is the vector connecting two successive hard sphere centers.

We are now in a position to describe chain formation and chain properties in a more quantitative way. The initial association of the dipolar spheres, starting from a face-centered-cubic lattice configuration with random orientations of the dipole moments, is generally quite fast. For example, at $\rho^* = 0.05$, after generating of the order of 5000 trial moves per particle, all particles were involved in a chain structure (no free monomers) and after 10 000 trial moves per particle, the mean chain length was already ~ 5. The evolution of the mean chain length l as a function of the number of Monte Carlo steps is shown in Fig. 5 for a 500 particle system at $\rho^* = 0.1$. A striking feature is its rapid fluctuation, indicating continuous breaking and recombination of the chains. In this respect it is tempting to qualify the chains as living polymers. The breakage-recombination process can occur through different mechanisms, the most obvious being combination of two chains when their ends meet to form a longer chain or, in the reverse case, breaking of a chain into two smaller chains. However, two other mechanisms previously invoked to describe the dynamics of living-polymer systems [10], end-interchange and bond-interchange reactions, seem to be operating as well and are possibly more efficient as lower energy barriers are involved. In the end-interchange reaction the end of one chain interacts with a second chain at some random position, causing the second chain to break into two sections at this point. The end of one of these sections then combines with the end of the first chain, while the other end remains free. A bond-interchange reaction can arise when two chains come into close contact at some point along their length. In this case two new chains can form through combination of a section of the first chain with

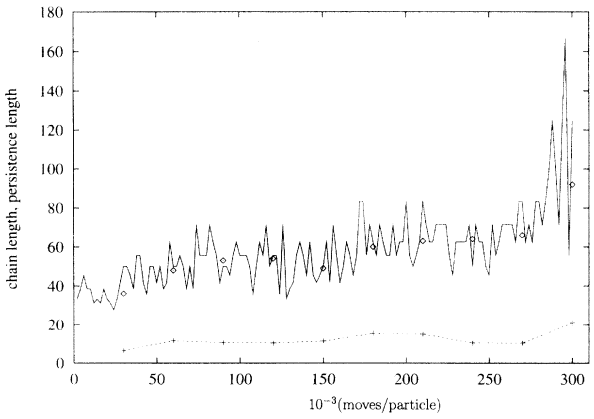

FIG. 5. Variation of the mean chain length l [Eq. (1)] as a function of the number of Monte Carlo steps for a system of 500 particles at $\rho^* = 0.1$ and $T^* = 0.0816$ (solid line). The diamonds and crosses represent, respectively, the average chain length $\bar{l}$ [Eq. (2)] and the average persistence length $\bar{l}_p/\sigma$ [Eq. (6)] calculated by averaging over blocks of configurations of 2.5×10^4 trial moves per particle (the dotted line merely connects the crosses).

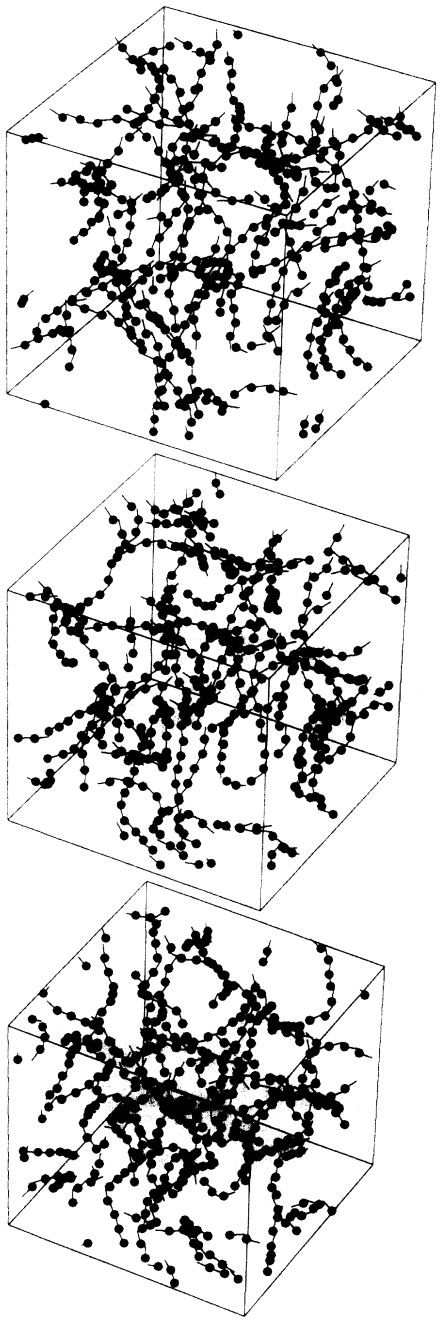

FIG. 6. Evolution of a system of 500 dipolar hard spheres at $\rho^* = 0.1$ and $T^* = 0.0816$ with the number of Monte Carlo steps. From top to bottom: snapshots of configurations after 10^5, 2×10^5, and 3×10^5 trial moves per particle. The box length is $L = 17.10\sigma$.

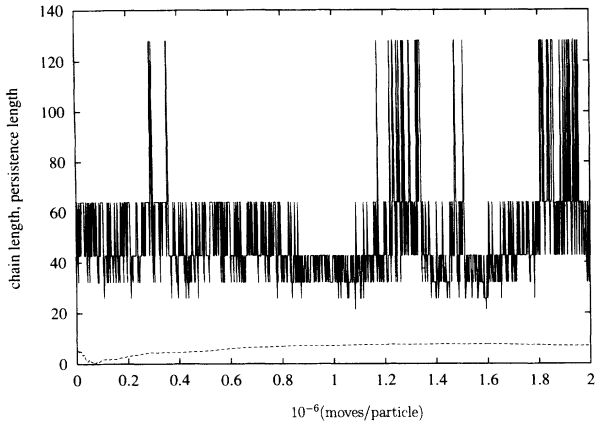

FIG. 7. Variation of the (instantaneous) mean chain length l [Eq. (1)] as a function of the number of Monte Carlo steps for a system of 128 dipolar hard spheres at $\rho^*=0.05$ and $T^*=0.0816$ (solid line). The dotted line represents the running average persistence length $\bar{l}_p/\sigma$ [Eq. (6)].

one or the other section of the second chain [10]. We did not investigate these mechanisms in detail.

A second, less pleasing, feature that is apparent in Fig. 5 is the slow but continuous increase of the mean chain length l, indicating the difficulty in obtaining equilibrium values even with sampling periods of the order of 300 000 steps per particle. However, snapshots of configurations of the system ($\rho^*=0.1$, 500 particles) after 100 000, 200 000, and 300 000 Monte Carlo steps per particle show (cf. Fig. 6) that even if the average length of the chains is slow to converge, the global structure of the system does not change qualitatively over this time span. They also show that on a local scale there is appreciable evolution of the system, giving significant credit to the simple sampling method used. The final configuration of the system at $\rho^*=0.1$ consists of four chains (taking into account the periodic boundary conditions) of lengths 203, 167, 106, and 24, respectively. The average chain length calculated over the block consisting of the last 100 000 steps per particle is 73 if Eq. (2) is used or 125 with Eq. (4). The persistence length averaged over the same block is $\bar{l}_p/\sigma \sim 13$.

In order to check whether an equilibrium state could be obtained by increasing the length of the simulation runs, we performed additional calculations for a 128 particle system at densities $\rho^*=0.01$ and 0.05. The smaller particle number allowed us to follow the evolution of the system over a time span of 2 million steps per particle. Analysis of the variation of the chain length with "time" at $\rho^*=0.05$ (Fig. 7) shows that after about 50 000 Monte Carlo steps per particle, the chain length fluctuates around an average value $\bar{l} \sim 50$. The persistence length averaged over the last million steps is $\sim 7\sigma$. For the density $\rho^*=0.01$, average chain lengths and persistence lengths are $\bar{l} \sim 45$ and $\bar{l}_p \sim 7\sigma$, respectively. Snapshots of configurations spaced by an interval of the order of a million Monte Carlo moves per particle are shown in Figs. 8 and 9 for $\rho^*=0.01$ and 0.05, respectively. Together with the 500 particle results, they allow for a number of conclusions: As already observed for the 500 particle system, there is considerable diffusion of the particles, giving support for the reliability of the sampling scheme. There is no evidence of the chains coiling, nor is there evidence for a tendency of the chains to separate into subvolumes of low and high densities; the spatial distribution of the chains seems fairly homogeneous. Rings can form occasionally, but are rare at the densities considered. The

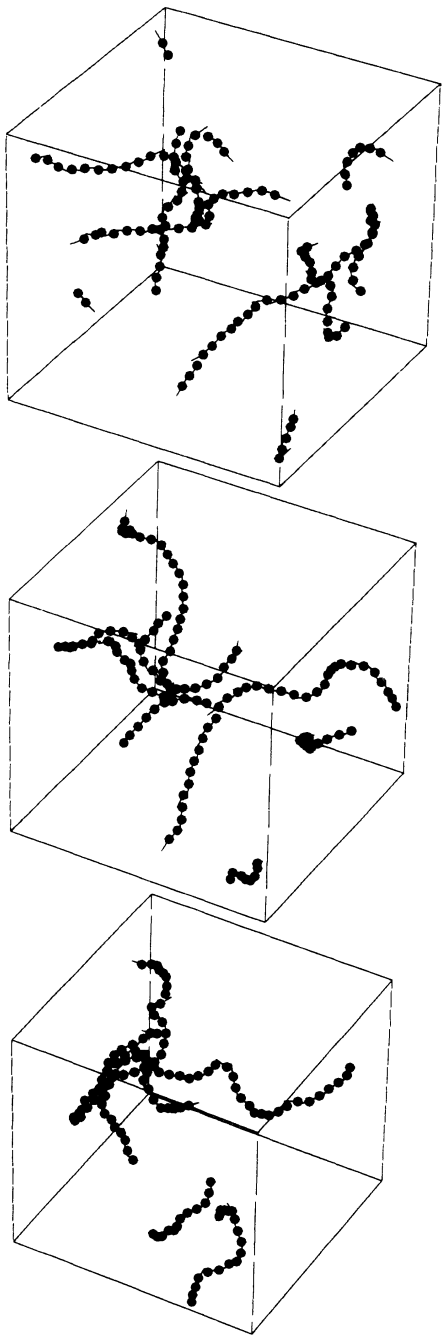

FIG. 8. Snapshots of the configuration of a 128 particle system at $\rho^*=0.01$ and $T^*=0.0816$ after (from top to bottom) 4×10^4, 1.4×10^6, and 2.4×10^6 trial moves per particle. The box length is $L=23.4\sigma$.

larger values of the chain lengths found for the 128 particle system, compared to those obtained for the 500 particle system at equal densities, indicate that a number of Monte Carlo moves of the order of $(1-3)\times 10^5$ moves per particle is not sufficient to guarantee a converged value of the chain length.

2. $\rho^* > 0.6$

Previous simulation studies have already shown that in this density region the system of dipolar hard spheres (as well as the related system of dipolar soft spheres) can exhibit, at sufficiently low temperatures, spontaneous orientational ordering of the dipole moments which, moreover, is ferroelectric [1,3]. We confirm this result for the temperature $T^*=0.0816$. A snapshot of a configuration at $\rho^*=0.8$ showing clear ferroelectric ordering is given in Fig. 10. The polarization of this thermodynamic state is $P=0.84$ (cf. Table I). The polarization $P=\langle P_1 \rangle$ is defined as the average value of

$$P_1=\frac{1}{N}\left|\sum_{i=1}^{N}\hat{\mathbf{u}}_i\cdot\hat{\mathbf{d}}\right|, \tag{7}$$

where $\hat{\mathbf{d}}$ is a unit vector in the direction of the (instantaneous) eigenvector associated with the largest eigenvalue P_2 of the second-rank tensor

$$\mathbf{Q}=\frac{1}{N}\sum_{i=1}^{N}\tfrac{1}{2}(3\hat{\mathbf{u}}_i\hat{\mathbf{u}}_i-\mathbf{I}) \tag{8}$$

and $\hat{\mathbf{u}}_i$ is a unit vector along the direction of the dipole moment of particle i. The usual nematic order parameter S is given by the average value of P_2. At the lower density $\rho^*=0.6$, a polarization $P=0.83$ was obtained starting from an initial perfectly polarized configuration (110 000 trial moves per particle). However, when the system was started from an unpolarized state with random distribution of the dipole moments, the polarization was extremely slow to build up and did not converge within the length of the run. The final value, after 110 000 trial moves per particle, was $P\simeq 0.30$.

3. $0.2<\rho^*<0.6$

In the intermediate density region an unambiguous characterization of the fluid structure is less straightfor-

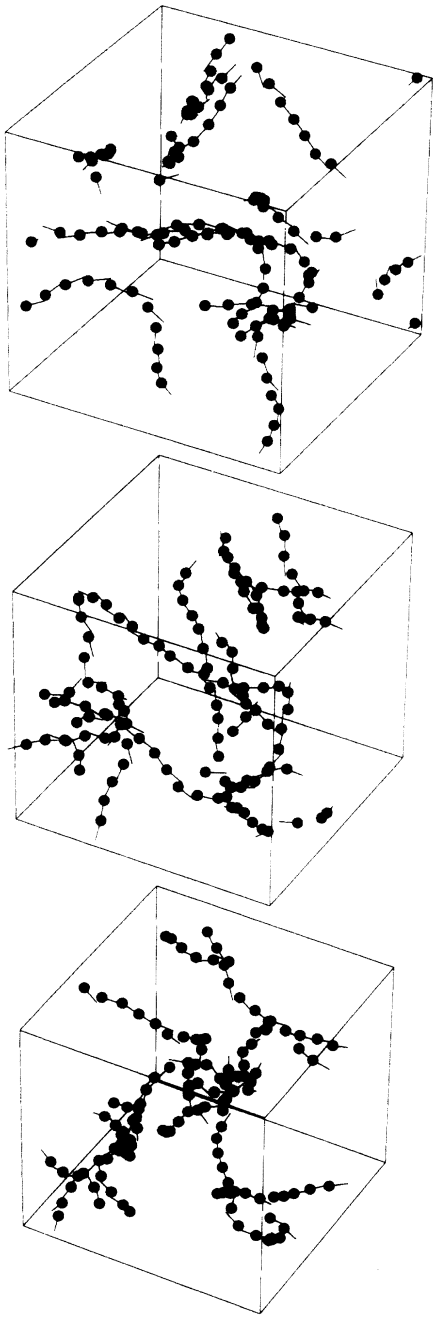

FIG. 9. Snapshots of the configuration of a 128 particle system at $\rho^*=0.05$ and $T^*=0.0816$ after (from top to bottom) 2×10^4, 10^6, and 2×10^6 trial moves per particle. The box length is $L=13.7\sigma$.

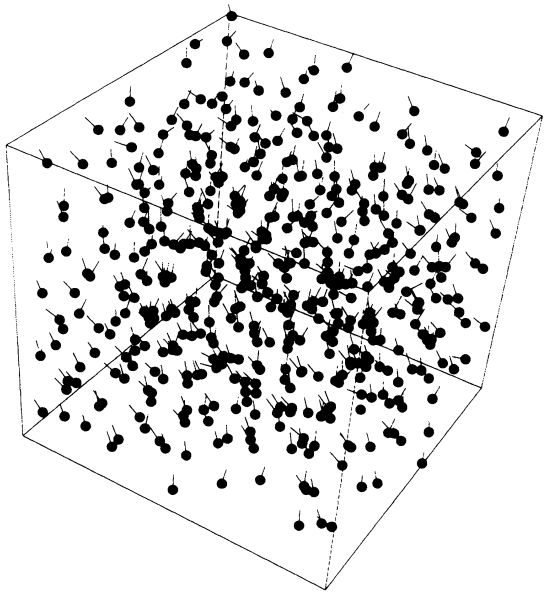

FIG. 10. Snapshot of a polarized configuration of 500 dipolar hard spheres at $\rho^*=0.8$, $T^*=0.0816$ (8×10^4 trial moves per particle). The direction of the dipole moments is indicated by a thin line. The box length is $L=8.55\sigma$.

ward than in the two previously discussed regions. This is due, on the one hand, to increased angular correlations between particles not just limited to the two next nearest neighbors and the resulting failure of a chain as defined above to be a useful concept and, on the other hand, to metastability of the polarization.

Snapshots of a 500 particle configuration at $\rho^*=0.4$ (after 110 000 steps per particle) and a 128 particle configuration at $\rho^*=0.5$ (after 2×10^6 steps per particle) are shown in Figs. 11 and 12, respectively. In both cases the initial distribution of the dipole moments was random. No net polarization developed in the system. However, when the simulation run at $\rho^*=0.4$ was started from a perfectly polarized initial configuration, the polarization was very slow to decay ($P\sim0.7$ after 110 000 Monte Carlo steps per particle), indicating large metastability effects.

The snapshots give no visible evidence of chain structures similar to those observable at lower density. If, nonetheless, we apply our chain criterion at density $\rho^*=0.4$, we identify "chains" with an average length of ~20. However, these "chains" are not stable entities involving well-defined particles as in the low density case; they merely reflect local orientational order in which dipole moments align with head-to-tail arrangement along some path. At these densities, a more refined description of orientational order, possibly based on order parameters similar to those used by Gringras, Holdsworth, and Bergersen [11] to identify local bond orientational order in hexatic smectic liquid crystals, is clearly in order.

Finally, from the preceding observations it is likely that the identification, in Ref. [5], of ferroelectric chains at density $\rho^*=0.3$ is an artifact of initial conditions (perfectly polarized configuration) and insufficient sampling of configuration space (40 000 trial moves per particle).

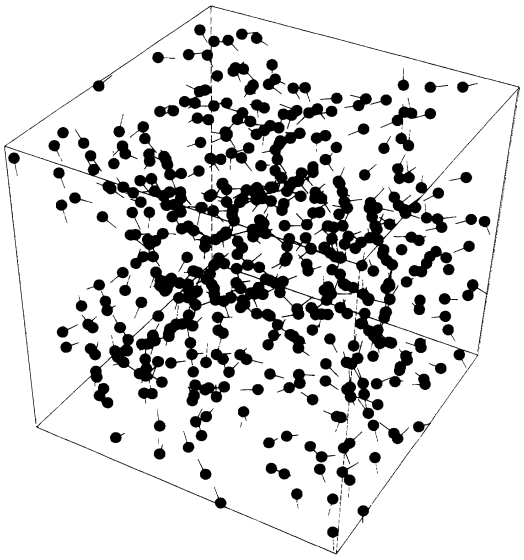

FIG. 11. Snapshot of a configuration of 500 dipolar hard spheres at $\rho^*=0.4$, $T^*=0.0816$ (1.1×10^5 trial moves per particle). The box length is 10.8σ.

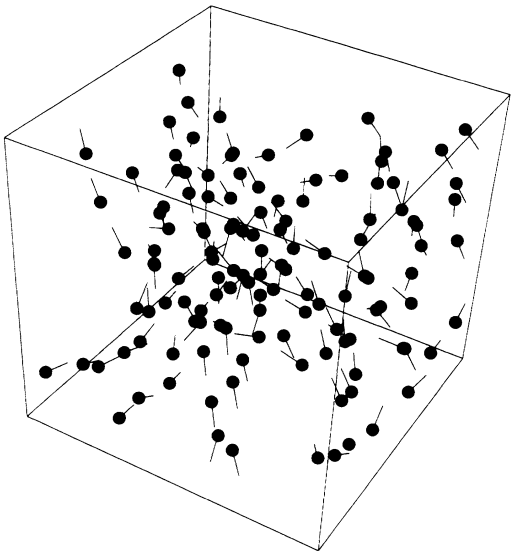

FIG. 12. Snapshot of a configuration of 128 dipolar hard spheres at $\rho^*=0.5$, $T^*=0.0816$ (2×10^6 trial moves per particle). The box length is 6.35σ.

B. Influence of boundary conditions

It is a well known fact that the orientational correlations in dipolar systems depend strongly on boundary conditions as a consequence of the long-range nature of the dipole-dipole interaction. A striking manifestation of boundary conditions is, for instance, the formation, in the ferroelectric phase, of domain structure when the system is subject to the depolarization field [1,4]. The influence on chain formation is less noticeable. The present simulation results at $\rho^*=0.1$ and 0.05, for a periodic system in vacuum and an isolated sphere in vacuum, respectively (cf. Sec. II), show that the effect is at best quantitative, and manifests mainly in a three to four times smaller persistence length and, probably, a somewhat smaller chain length compared to the case when $\epsilon'=\infty$. This lower value of l_p is likely to result from an increased flexibility of the chains due to a weakening, induced by the depolarizing field, of the alignment of neighboring dipoles. A precise comparison seems not to be feasible due to possible lack of convergence of these quantities, but an order of magnitude estimate of the difference can be made. For example, at $\rho^*=0.1$, we find $\bar{l}_p\sim3$ and $\bar{l}\sim30$ ($\bar{l}_s\sim60$) for the periodic system in vacuum (500 particles, 100 000 moves per particle) compared to $\bar{l}_p\sim12$ and $\bar{l}\sim60$ ($\bar{l}_s\sim100$) for the periodic system without boundary (500 particles, 300 000 moves per particle). Similarly, at $\rho^*=0.05$, the values for $\bar{l}_p$ and $\bar{l}$ are 1.6 and 25, respectively, for a sphere in vacuum (2046 particles, 70 000 moves per particle) and 7 and 50 for the infinite periodic system (128 particles, 2×10^5 moves per particle). The snapshot of a configuration of the 2046-particle system is shown in Fig. 13. One notes the preference of the chains to order parallel to the surface near the spherical boundary. This arrangement is in agreement with the earlier observation, made at higher temperatures, that dipolar hard spheres orient their dipole moment with high probability parallel to an inert hard wall [12].

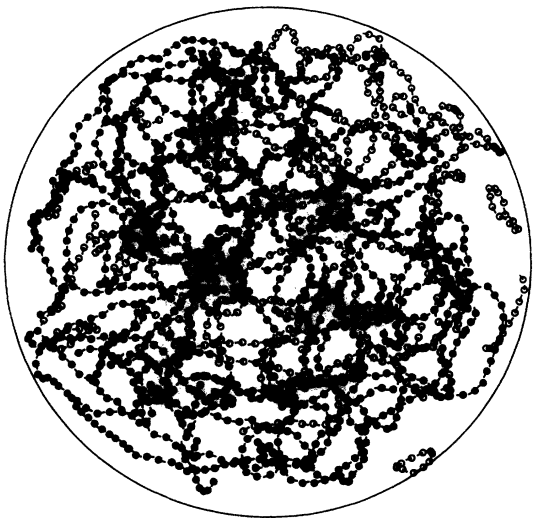

FIG. 13. Snapshot of a configuration of 2046 dipolar hard spheres in a spherical volume in vacuum (see the text). All the particles are projected on an equatorial plane. Hard spheres belonging to chains with length larger than 50 are represented in black, the others in gray. The radius of the confining sphere is 21.4σ.

C. Variation with temperature

The structural changes entailed by a temperature increase are best perceived by comparing snapshots of configurations obtained at a series of different temperatures. An example is given in Fig. 14 for the density $\rho^*=0.1$. Upon increase of temperature, the average chain length progressively diminishes (cf. Table I of Ref. [5]). A rapid increase in the number of free monomers occurs near $T^*=0.25$ ($\sim$200 monomers). However, at this temperature half of the particles still partake in small short-lived structures involving two to three particles with nearly aligned dipole moments. Similar behavior has been found to occur at $\rho^*=0.02$ and 0.3 [5].

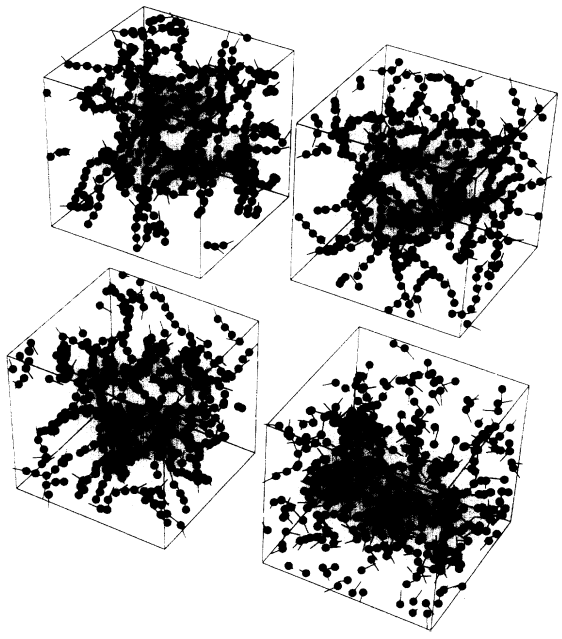

FIG. 14. Variation with temperature of the structure of a system of 500 dipolar hard spheres at $\rho^*=0.1$. From left to right and top to bottom the temperatures are $T^*=0.0816$ ($\mu^*=3.5$), 0.111 ($\mu^*=3$), 0.16 ($\mu^*=2.5$), and 0.25 ($\mu^*=2$), respectively. The box length is 17.10σ.

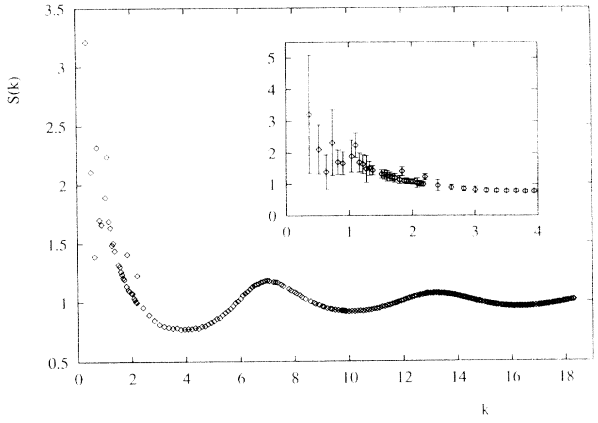

FIG. 15. Orientationally averaged structure factor of the dipolar hard sphere system (500 particles) at $\rho^*=0.1$, $T^*=0.25$. k is in units of σ^{-1}. The low k values of $S(k)$ are shown in the inset with their estimated standard errors. The standard errors were calculated by dividing the simulation run into 150 blocks, corresponding to 2000 moves per particle, each. The reliability of the estimates of the variance, σ_k^2, obtained, for each k, from the 150 $S(k)$ values was checked by computing the relaxation functions associated with the $S(k)$ values. These functions show that for $k\sigma>2$, values of $S(k)$ are correlated over $\sim 10^4$ moves per particle and, for $k\sigma\leq 1$, over 10^5 moves per particle. From these results we infer a standard error of $\sim$0.02–0.03 for $k\sigma\geq 2$ where $\sigma_k\sim 0.2$, but for $k\sigma\sim 1$ the standard error is of the order of σ_k.

These structural changes are also apparent from the angle averaged structure factors

$$S(k)=\left\langle \sum_{\substack{i,j=1\\ i\neq j}}^{N} e^{i\mathbf{k}\cdot(\mathbf{r}_i-\mathbf{r}_j)} \right\rangle \tag{9}$$

shown in Figs. 15 and 16 for $\rho^*=0.1$ and the two tem-

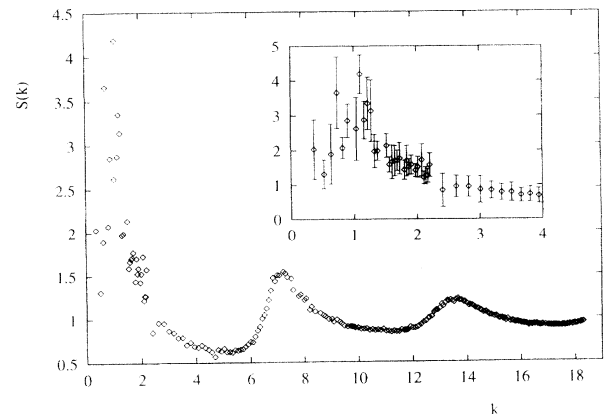

FIG. 16. Orientationally averaged structure factor of the dipolar hard sphere system (500 particles) at $\rho^*=0.1$, $T^*=0.0816$. k is in units of σ^{-1}. The analysis of the error estimate is similar to that given in Fig. 15.

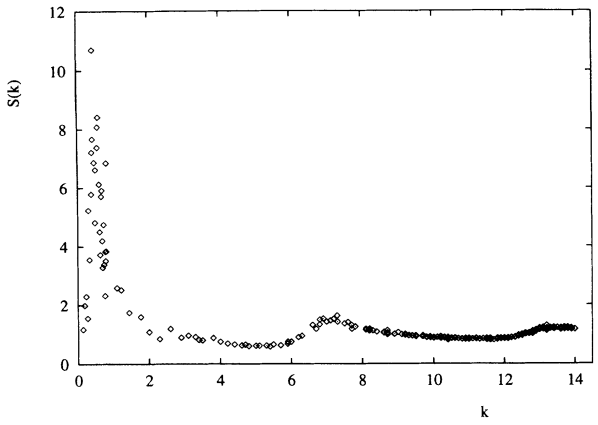

FIG. 17. Orientationally averaged structure factor of the dipolar hard sphere system (500 particles) at $\rho^*=0.005$, $T^*=0.0816$. k is in units of σ^{-1}. For this run of 10^5 trial moves per particle, no reliable estimate of the error bars could be obtained for $k\sigma \leq 2$ because of the slow decrease of the relaxation functions associated with the block estimates of the $S(k)$ values.

peratures $T^*=0.0816$ and 0.25 ($\mathbf{k}$ is the reciprocal lattice vector of the cubic simulation cell, $k=|\mathbf{k}|$).

Despite considerable statistical noise for $k\sigma \leq 2$, $S(k)$, at $T^*=0.25$, is easily recognized to be a monotonically increasing function at low k, typical of the behavior of a homogeneous dipolar fluid, whereas at $T^*=0.0816$, it has a pronounced first peak at $k\sigma \sim 1$. This peak is primarily due to intermolecular scattering by the chains, but its position and height may be modified by intramolecular contributions [13]. The lower value of $S(0)$ at $T^*=0.0816$, compared to the high temperature case, attests to the lower compressibility of the system as a result of association of the particles into chain structures. As the density is lowered (at $T^*=0.0816$), the position of the first peak is shifted to lower k values in accordance with the larger intermolecular spacing of the chains (cf. Fig. 17). Finally, we can remark that chain formation is also reflected in the asymmetrical shape of the second and third peaks of $S(k)$.

IV. CONCLUSION

In spite of extensive Monte Carlo simulations, in which configurations of the system evolve considerably, the conclusions of the present work concerning the nature of the equilibrium states of low temperature dipolar hard spheres remain qualitative and partly conjectural. The results that appear most certain belong to the two density domains $0.005<\rho^*<0.2$ and $\rho^*>0.6$ up to the solid phase transition. In the first domain, clearly, the molecular arrangement is characterized by association into chainlike structures which are easily identifiable by simple visualization of the configurations. Furthermore, for the finite systems considered in our simulations, the transition from the dilute homogeneous fluid state at high temperature to the state of association into chains at low temperature is progressive and continuous and occurs in the temperature range $T^*=0.11-0.16$. However, since a precise calculation of the thermodynamic properties has not been obtained, the nature of this transition (continuous, second order, etc.) remains uncertain.

The difficulty of sampling configuration space, when the molecules have grouped into chains, arises from the fact that chains can grow or break only through interaction, in close encounters, between segments of different chains (cf. Sec. III), or between segments of the same chain which, on account of the rigidity of the assemblage, are far apart. This difficulty is manifested quantitatively in the value of the statistical error affecting $S(k)$ at $k\sigma \leq 1$. It is possible that a more efficient sampling of the relative positions of the chains could be achieved by performing *a priori* moves on an entire chain, the chain entity being defined by the algorithm described in Sec. III. The efficiency of such a procedure has, however, not been explored in the present work.

An important remark concerns the spatial distribution of the chains: In none of our simulations has evidence been obtained for a density inhomogeneity associated with a concentration of chains in some subvolume of the simulation volume, indicating possible coexistence between a density-rich and a density-poor chain arrangement. In contrast, such inhomogeneities are easily observed in systems having a liquid-gas transition such as, for example, the continuum Heisenberg model [14]. The uniform arrangement of the chains is evidently in agreement with the results of Refs. [6,7] which point to the absence of a liquid-gas transition in the dipolar hard sphere system.

For densities $\rho^* \ll 0.005$ and $T^* \leq 0.05$, the exact nature of the equilibrium states remains problematic; in particular, the stability of the chain structures has not been investigated in this range of thermodynamic states.

Thermodynamic states with density $\rho^*>0.6$ and $T^* \sim 0.1$ have been described in detail in Refs. [1,4]; they present an order-disorder type transition towards an ordered phase characterized either by a net polarization of the system or, in the presence of a depolarization field, by the formation of domains polarized in different directions such that the global polarization of the system vanishes. In this density domain the chain definition given in Sec. III is clearly unrealistic: Indeed, if it is still possible to associate the molecules in a nearby linear way using the two lowest energies of neighboring molecules, these arrangements have a very reduced stability ($\ll 1000$ moves per particle). An analysis of the correlations between the orientations of the dipole moments and the positions of the molecules, similar to the one proposed in Ref. [11], could possibly give a more adequate description of the structural order of the system in this density domain.

For densities $\rho^* \sim 0.2-0.6$ and $T^* \leq 0.1$, our results do not permit us, at present, to give a precise description of the transformation of the low density chain states into dense polarized fluid states. In particular, the location of the line of Curie points of the order-disorder transition is unknown. This is, partly, a consequence of considerable metastability which impedes a precise evaluation of the polarizability within acceptable computer times.

The simplest conjecture for the low temperature phase diagram of DHS is that of a polarized fluid whose line of

Curie points terminates at $T^*=0$ and $\rho^* \geq 0.4$. In addition, the states with $\rho^* \leq 0.4$ and $T^* \leq 0.15$ are characterized by the progressive appearance of an organization of the molecules into chain structures, this organization being complete only for $\rho^* \leq 0.2$ and $T^* \leq 0.1$. However, the existence of phase coexistence, in relation with a first-order phase transition, seems to be ruled out by our results.

A firm and unambiguous result in this region of the phase diagram is the value of the internal energy per particle. For instance, at $T^*=0.0816$, its value, $-25(\simeq -2\mu^{*2})$ remains constant (within 10%) for a density variation of two orders of magnitude from 0.005 to 0.4. This value also indicates that correlations between three nearest neighbors associated linearly are dominant and should be taken into account explicitly in a theoretical calculation of the equation of state of DHS at low temperature. The difficulties of such an approach are stressed, for instance, in Ref. [15].

ACKNOWLEDGMENTS

We acknowledge with pleasure discussions with Mike Widom, George Stell, and Margarida Telo de Gama. The Laboratoire de Physique Théorique et Hautes Energies is "associé au Centre National de la Recherche Scientifique."

[1] D. Wei and G. N. Patey, Phys. Rev. Lett. **68**, 2043 (1992); Phys. Rev. A **46**, 7783 (1992).
[2] D. Wei and G. N. Patey, Phys. Rev. E **47**, 2954 (1993).
[3] J. J. Weis, D. Levesque, and G. J. Zarragoicoechea, Phys. Rev. Lett. **69**, 913 (1992).
[4] J. J. Weis and D. Levesque, Phys. Rev. E **48**, 3728 (1993).
[5] J. J. Weis and D. Levesque, Phys. Rev. Lett. **71**, 2729 (1993).
[6] J. M. Caillol, J. Chem. Phys. **98**, 9835 (1993).
[7] M. E. Van Leeuwen and B. Smit, Phys. Rev. Lett. **71**, 3991 (1993).
[8] See, e.g., M. P. Allen and D. J. Tildesley, *Computer Simulations of Liquids* (Clarendon, Oxford, 1989).
[9] P. G. de Gennes and P. A. Pincus, Phys. Kondens. Mater. **11**, 189 (1970).
[10] See, for instance, M. E. Cates and S. J. Candou, J. Phys. Condens. Matter **2**, 6869 (1990); M. S. Turner and M. E. Cates, J. Phys. II (France) **2**, 503 (1992).
[11] M. J. P. Gringas, P. C. W. Holdsworth, and B. Bergersen, Phys. Rev. A **41**, 6786 (1990).
[12] D. Levesque and J. J. Weis, J. Stat. Phys. **40**, 29 (1985).
[13] A. H. Narten, A. Habenschuss, K. G. Honnell, J. D. McCoy, J. G. Curro, and K. S. Schweizer, J. Chem. Soc. Faraday Trans. **88**, 1791 (1992).
[14] E. Lomba, J. J. Weis, N. S. Almarza, F. Bresme, and G. Stell, Phys. Rev. E **49**, 5169 (1994).
[15] P. C. Jordan, Mol. Phys. **38**, 769 (1979).